USING SEASEEP SURVEYS TO IDENTIFY AND SAMPLE NATURAL HYDROCARBON SEEPS IN OFFSHORE FRONTIER BASINS

Daniel L. Orange*
Philip A. Teas*
John Decker*
Peter Baillie**
Tanya Johnstone**

ABSTRACT

SeaSeep surveys are designed to rapidly and efficiently identify offshore frontier basins that have hydrocarbon charge and working petroleum systems. The SeaSeep approach combines traditional exploration techniques with the less traditional tools of high-resolution multibeam sonar and targeted sea-bottom cores. Multibeam (a mapping tool developed by the US defense industry that was declassified in the 1970s and is widely used in the hydrographic survey industry) is an ideal tool for detecting sites of potential seafloor hydrocarbon seepage because the presence of seep-related biologic communities and authigenic carbonate or gas hydrate alters the acoustic properties, and sometimes the shape, of the seafloor.

Over 1000 sq km per day of high resolution multibeam data were acquired in water depths of 400-3000 m as part of the TGS Indonesia Frontier Basins (IndoDeep) multi-client project. Because seafloor seeps can be small, high resolution data combined with accurate core positioning are required. Accurate core placement is accomplished by USBL tracking of the piston cores in real time, allowing the core barrel to be placed on the seafloor within meters of the intended target. Cores are then sub-sampled for detailed geochemical analysis to determine the amount and type of hydrocarbons that may be present.

TGS-NOPEC Geophysical Company (TGS) has mapped over 400,000 sq km and acquired 1182 cores for geochemical analysis in Indonesia. These data were combined with 2D seismic, gravity, magnetic and heatflow data to identify a basin's structural elements, potential hydrocarbon kitchens and leads. By integrating these with the core geochemistry, Black Gold Energy was able to focus on the parts of the survey areas that warranted further exploration effort.

INTRODUCTION

Exploring for oil and gas, particularly in remote deepwater basins, is an expensive proposition. In order to justify such expenses, exploration companies are keenly interested in reducing exploration risk. Most of Indonesia's remote offshore basins remain underexplored with insufficient data acquired to demonstrate a functioning petroleum system. As a result, many exploration companies have not bid on blocks offered in these basins.

To further evaluate the hydrocarbon potential of Indonesia's frontier offshore basins, Black Gold Energy LLC (BGE) and its subsidiaries underwrote the acquisition of the TGS Indonesia Frontier Basins (IndoDeep) multi-client project (Figure 1). SeaSeep exploration formed the backbone of the IndoDeep project, and refers to a rapid and cost effective survey approach combining multibeam sonar, piston coring, traditional 2D seismic, gravity, magnetics, and heat flow measurements.

NATURAL SEAFLOOR HYDROCARBON SEEPS

The primary goal of SeaSeep exploration is to identify locations of potential natural hydrocarbon seafloor seeps to be sampled by surface-deployed piston cores. The cores can then then analyzed geochemically for the signature of natural hydrocarbons.

Natural seafloor hydrocarbon seeps can alter the physical and biological characteristics of the sediment-water interface (Figure 2; Suess et al.,

---

*   Black Gold Energy LLC
**   TGS-NOPEC Geophysical Company

1985; Kennicutt et al., 1985; Kulm et al., 1986). Specifically, the presence of seep-related biologic communities and authigenic carbonate or gas hydrate can increase impedance (hardness; Roberts et al., 1990), roughness, and volumetric heterogeneity several meters below the seafloor at seep sites, and all increase the backscatter energy recorded by the multibeam system (e.g., Orange et al., 1999, 2002; Fonseca et al., 2002; Somoza et al., 2003). Seepage can also lead to local bathymetric highs (mounds, mud volcanoes), and lows (pock marks), and seepage may occur along bathymetrically expressed fault lineaments (Hovland and Judd, 1988; Le Pichon et al., 1990; Roberts et al., 1990; Orange et al., 1999, 2002; Sager et al., 2003, 2004; Judd and Hovland, 2007).

IDENTIFYING POTENTIAL SEEP TARGETS

Until recently, there have been no means to survey the seafloor beyond the shelf with sufficient accuracy or resolution to image hydrocarbon seeps in a cost-effective manner. Natural marine hydrocarbon seepage is of a similar scale to terrestrial examples, as demonstrated by submersible (MacDonald et al., 1989) and remote operated vehicle (Orange et al., 1999) dives, which documented active seafloor seeps to be from tens of meters to 100 m across. The declassification of the US Navy's multibeam technology provided the first big step in seafloor mapping technology, as it allowed the non-government user to survey a swath of the seafloor instead of the area directly below the vessel (e.g., single beam, Mayer, 2006).

Multibeam uses a pair of orthogonal acoustic arrays to image a swath of the seafloor (Figure 3; Steinberg, 1976; Stutzman and Thiele, 1981). Today's highest resolution multibeam systems have transmit and receive arrays that create beams 1-2° across with over 200 beams and a total mappable swath up to a 150° across. In addition, significant improvements in attitude sensing systems (motion reference units, or MRUs), have led to much higher quality orientation information for the vessel, and readily available differential Global Positioning System (D-GPS) navigation systems have lead to improvements in vessel positioning. The combination of these, plus advances in multibeam sonar system resolution and quality water column measurements to correct for refraction, has lead to a significant improvement in multibeam resolution.

Bathymetric data alone, however, can not identify all possible hydrocarbon seeps, because many hydrocarbon seeps have no bathymetric expression (e.g., Orange et al., 1999, 2002),. Seep communities and their associated precipitates, however, can increase the hardness and roughness of the seafloor, and if buried below the mud line, can increase the volumetric heterogeneity of the shallow section, similar to lava flows (Gardner et al., 1991), and turbidites and mass transport complexes (Kenyon, 1992). One or more of these (seafloor hardness, seafloor roughness, volumetric heterogeneity), can increase the backscatter intensity recorded by the multibeam system. All of the beams recorded during a survey are assembled to give the backscatter variation across the entire swath of insonified energy (Figure 3). By tying the backscatter within each beam to that beam's location on the seafloor, the result is georeferenced quantitative backscatter (in addition to georeferenced bathymetry), now at a scale relevant to identifying hydrocarbon seepage in the marine environment (Orange et al., 2008).

SAMPLING POTENTIAL SEEP TARGETS

Ultra-Short BaseLine (USBL) navigation systems were used to track the position of the core through the water column. Similar to multibeam, larger USBL transducer arrays allow for a narrower beam angle, and tighter discrimination of an object's position in the water column. The position of the core is tracked in real time in GIS via a serial cable connection from the ship's navigation computer. The piston core can be tracked from the surface to the seafloor with a very high degree of accuracy (1%, to perhaps 0.5%, of water depth), which is sufficient to target small coring objectives identified from the multibeam (Figure 4).

Piston coring was used to sample features of interest. The routine core length was 6 m, although longer cores up to 9 m were acquired for stratigraphic data. The recovered cores were visually examined at the surface for indications of hydrocarbons (for example, gas hydrate, gas parting, or oil staining) and then sub-sampled for geochemical analysis.

One-third of each sub-section was used to sample for interstitial gases. These samples were placed into 500 mL cans and covered with 165 mL of clean, degassed seawater with bactericide added. The cans were quickly purged with nitrogen gas to remove atmospheric gases before sealing. All samples were frozen at -20° C. Every effort was made to minimize the time between core retrieval, sample processing, and frozen sample storage. One-third of each sub-section was extruded directly

into labeled plastic bags for sediment extract analyses. The remaining one third of each sub-section was bagged and retained as an archive / replicate sample, which was retained on the ship until confirmation that the first set had been received by the geochemistry laboratory.

Geochemical analyses included: (1) total scanning fluorescence (TSF) spectra from bagged sediment sections using dried-sediment solvent extraction, (2) gas chromatography for the C_{15+} hydrocarbon concentrations in the same sediment extracts, and (3) head-space gas analysis of the interstitial light hydrocarbon gas (C_1-C_5) concentrations from separately canned sediment sections using wet-sediment gas partitioning and gas chromatography. From these analyses, screening indicators of migrated liquid and gaseous thermogenic hydrocarbons were developed and used to qualify cores and distinguish them from defined background thresholds for the study area (for a thorough discussion of the IndoDeep geochemical analysis program and protocol, see Bernard et al., 2008).

RAKSASA (GIANT) MUD VOLCANO

Multibeam data acquired in the far southwestern Moluccas imaged a very large mud volcano (Figure 5a) approximately 35 km southeast of Pulau Lakor. This feature is circular in map view, 12 km in diameter at the base, 6 km in diameter at the crest, and rises 350 m above the surrounding seafloor. Concentric but discontinuous ridges characterize the slope of the mud volcano, with a sharp contact at the base of the mud volcano suggesting a young geologic feature. Smaller apparent mud volcanoes and a large pock mark surround the main mud volcano.

The central portion of the crest of the mud volcano is continuously high backscatter, with the high backscatter interspersed with concentric but discontinuous small elongate areas of low backscatter toward the margin of the crest (Figure 5b). Note that the prominent east-west backscatter stripes across the mud volcano and surrounding seafloor are due to a near-nadir artifact inherent to the geometry and processing of multibeam backscatter.

The pockmark to the WNW of the large mud volcano (dotted circle) shows no significant high backscatter anomaly. In contrast, a small mud volcano to the south (dot, arrow) shows extremely high backscatter in a raised area within a central depression.

A composite mud volcano complex to the WSW (dashed circle) shows a more complex bathymetric and backscatter signature. This complex includes a small, sharp relief mud volcano to the SSE of the complex (Figure 5a) that shows no backscatter anomaly (Figure 5b), in contrast to the smoother larger mud volcano feature here that shows very high backscatter on the positive relief, and elongate tongues of high backscatter emanating away from the area of high relief. We interpret these tongues to be relatively recent (within 10 m of the mudline) mud flows that have erupted from the main mud volcano edifice here, making this a more promising site for hydrocarbon geochemical sampling than the more sharp (younger appearing) mud volcano.

A seismic line across the Raksasa mud volcano (Figure 5c) clearly images the entire mud volcano body, based upon the depressed reflectors below it that project to the undeformed strata to the north. The base of the mud volcano appears to be bulbous on this seismic line, extending to 1.5 sec two-way travel time below the crest. The depressed reflectors suggest subsidence following extrusion of the mud volcano material on the order of 1.1 sec below the maximum diameter. Within the central part of the mud volcano there is relatively little coherent seismic energy, although a negative polarity reflector suggestive of a bottom simulating reflector (interpreted to represent the base of the hydrate stability field with free gas below; Shipley et al., 1979; Hyndman and Spence, 1992; Xu and Ruppel, 1999; Mosher, 2008; Westbrook et al., 2008) is visible in the central area 300 ms below the seafloor. The northern flank of the mud volcano is similarly devoid of internal character, yet the southern flank shows northward dipping sub-surface reflectors. The combination of these reflectors, and the seafloor morphology suggestive of a stacked fold belt at the flank of the mud volcano, lead us to interpret these reflectors as separating discrete intervals of mud extrusion.

Identifying, Prioritizing, and Sampling Features of Interest

Anomalous bathymetric and backscatter features are identified on the multibeam data, and where possible, tied to the subsurface architecture using seismic data. Individual targets are described based upon their observed features (relief, backscatter, lineations, seafloor structural culminations, etc.), and interpreted based upon their geomorphic character (e.g., Figure 5). Targets are graded by each interpreter based upon perceived quality (e.g., potential for hydrocarbons) as well as their potential

impact on the prospectivity of a basin. Cores are also placed over identified leads and possible seafloor leak points.

To generate a set of targets to be sampled, we select a range of target types spread across the entire area of interest, and then prioritize these such that at the end of the coring program we have adequately sampled the survey area. Our strategy is to spread targets spatially, so that all parts of a survey area are interrogated.

Note that we also acquire cores in benign parts of a survey area for background geochemical information and regional sedimentology, and surface heat flow data.

Four cores were acquired in the Raksasa mud volcano (see dots, Figure 5). Three cores were acquired on the crest of the mud volcano, two in close proximity, and one several kilometers away. All three were on anomalously high backscatter anomalies. The geochemical signature of these three cores is remarkably consistent (e.g., TSF of 155000, 181000, and 174000 units; anomalous C1-C5 in all cores; and $\delta^{13}C_1$ = -32‰ $\pm$ 1‰, $\delta^{13}C_2$ = -25‰ (all 3), and $\delta^{13}C_3$ = -22‰ $\pm$ 1‰), indicating a common source for the interpreted oil and thermogenic gas. In contrast to these three, a core from the small mud volcano to the south yielded no significant C2-C5, an isotopically lighter $\delta^{13}C_1$ = -66‰ and $\delta^{13}C_2$ = -31‰, and a weaker TSF of 38000 units. Although this core passed threshold values for both oil and gas, we suggest that at this site a deep source fluid may be mixing with a more shallowly sourced biogenic gas en route to the surface (see location of all three crestal cores projected onto a seismic line through the mud volcano, and the small mud volcano directly on the seismic line, in Figure 5c).

TANNINBAR TROUGH

Small, subtle targets that have no anomalous bathymetric relief are common in the IndoDeep survey. Figure 6 shows a portion of the Tanninbar Trough southeast of the island of Jamdena characterized by an irregular and steep southeast facing slope, an undeformed and monotonous seafloor to the southeast, and a subtle toe-of-slope anticline between them. No obvious mud volcanoes

or anomalous seafloor seep targets are identified on the bathymetric data (Figure 6a).

The backscatter mosaic, however, shows numerous small patches of anomalously high backscatter. Several high backscatter patches occur along the crest of the anticline, and two of these were targeted for sampling (see Figure 7 for a close-up of the central feature). A third anomalous backscatter patch, occurring above the first deformed ridge, was also sampled. Anomalously high backscatter patches within the more deformed region occur as isolated patches as well as elongate patches along interpreted high angle fault zones. Note also that two isolated high backscatter patches occur on the undeformed region to the east and southeast. Geochemical data from all three sampled sites indicate the presence of thermogenic gas, although all have a biogenic overprint as indicated by the carbon isotopes.

NORTH MAKASSAR BASIN

Multibeam bathymetry and backscatter data showed a number of targets in the North Makassar basin, an area that previously had been surveyed by only 2D seismic data (Figure 8). Anomalous backscatter potential seep features occur both on undeformed seafloor with no relief, and along features with bathymetric expression such as faults and fault-related anticlines. It is important to note that even on features with seafloor bathymetric expression the anomalous backscatter is not present along the entire feature, but instead on localized portions of the feature. We interpret these backscatter anomalies to indicate where, on a geologic feature that may be controlling seepage, the actual seepage may have occurred in the recent geologic past.

Eight cores were dropped in the approximately 500 sq km area shown in Figure 8 (see dots and arrows): four cores targeted anomalous backscatter patches away from seafloor bathymetric features, two cores targeted anomalous backscatter patches on faults with seafloor expression, and one core targeted an anomalous backscatter patch on a hanging-wall anticline above a fault with seafloor expression. All three target types yielded evidence of hydrocarbons. The geochemical signature within each target type was similar, but there were differences between the target types in terms of the detailed geochemistry, and in the strength of the anomalous geochemical returns.
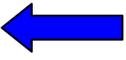
Similar target types occur elsewhere in the survey area that were not cored (Figure 8b). However, reasonable interpretations of these features can be made by analogy with the sampled features, thereby reducing the need to sample every feature within a survey for maximum cost efficiency.

MUD VOLCANO TARGETS IN THE INDODEEP PROGRAM

High Backscatter Targets with Variable Relief

Mud volcanoes were identified in numerous sub-areas in the IndoDeep program (Figure 9). Mud volcanoes vary widely in terms of their shape and rugosity. In some areas (Figures 9a and 9b), mud volcanoes occur as composite features with multiple seafloor highs. In other areas (Figure 9c), they occur as circular features with flat tops, whereas in other areas they can be conical (Figure 9d). High backscatter associated with mud volcanoes can occur across the entire crest of the feature (Figures 5b, 9c and 9d), or they can occur on only portions of the feature (Figures 9a and 9b). As in Figure 5b, some mud volcanoes show tongues of anomalously high backscatter emanating away from the central high which follow local subtle lows on the seafloor. We interpret these as relatively recent (within 10 m of the seafloor) mud flows away from the main extrusion zone. Figure 9d shows two mud volcanoes, both with interpreted mud flows. The southeastern feature showed higher backscatter, and was therefore targeted for sampling.

All of the mud volcanoes shown in Figure 9 yielded hydrocarbons. The two samples obtained on the mud volcano in Figure 9b were remarkably consistent, whereas the two samples from Figure 9a showed differences in the strength of the hydrocarbon anomalies. Sufficient material for biomarker analysis was obtained on the mud volcanoes in all except Figure 9b; the biomarkers, however, are notably different between different survey areas, and demonstrate that different petroleum systems (e.g., Mesozoic vs. Tertiary; Klasafet-type vs. carbonate) are active in different parts of the survey area (see Noble et al., 2009; this volume).

High Backscatter Chemosynthetic Community

In the Misool survey area, the multibeam survey revealed a broad ridge plunging gently to the ENE, with a long, gently sloping NNW limb and a shorter, more steeply sloping SSE facing limb (Figure 10a). Near the crest of the ridge several high backscatter patches were imaged that were several hundred meters across each, most with no associated anomalous bathymetry (Figure 10b). A piston core placed in the middle of the anomalous backscatter patch shown in Figure 10b recovered numerous whole live chemosynthetic mussels (*Bathymodiolus sp.*? mytilid mussels), numerous shell fragments, some authigenic carbonate, but no sediment (Figure 10c). A box core was deployed to the piston core location, and, using the USBL navigation, was placed in the seafloor within meters of the piston core location. This box core recovered hundreds of live chemosynthetic mussels (two possible species?) and pogonopheran tube worms as well as more cosmopolitan species such as galatheid crabs and brittle stars.

A seismic lines crosses this ridge, and shows a patchy bottom simulating reflector (BSR), interpreted to represent the base of the hydrate stability field, that is locally elevated beneath the crest of the ridge and shows increased local brightening below it as well as occluded imagery suggestive of gas clouds (Figure 10d). We interpret the shoaling of the BSR to be due to fluid and heat transport from depth (Zwart et al., 1996), the local brightening of the sub-BSR section to be due to an increase in local gas content below the BSR (McConnell and Kendall, 2002; Mosher, 2008; Westbrook et al., 2008), and the acoustic turbidity to be due to gas in the section (Fleisher at al., 2001; Hovland and Judd, 1988; Judd and Hovland, 2007).

On the NW limb two core samples retrieved showed evidence of both gas and oil, and are shown projected onto the seismic line in Figure 10d. The seafloor morphology suggests that these sites may in part have fluid expulsion associated with faults with seafloor expression, as well as a local headscarp that may facilitate geomorphic focusing of fluid flow (e.g., Robb, 1984, 1990; Orange and Breen, 1992).

High Backscatter Tear Faults

Elsewhere in the Misool survey area, the multibeam survey imaged a NE-trending anticline that, along strike, projects into two parallel NE-trending anticlines (Figure 11a). The multibeam bathmetry shows that the geomorphically sharp boundary is on the northeast side of the pair of anticlines, and the NE side of the region where the anticlines merge along strike, but that there is no sharp boundary on the southeastern single anticline. Where it can be interpreted, therefore, these anticlines appear to be NW-vergent.

The backscatter mosaic shows that there is a portion of the seafloor, where the single anticline projects into the two anticlines, that is characterized by anomalously high backscatter (Figure 11b). The high backscatter is patchy to elongate, and oriented NNE. Upon close inspection of the bathymetry, the high backscatter appears to be related to a set of subtle fault lineations that obliquely cut the anticlinal ridgecrest. These fault lineations are present away from the anticlinal ridge crest, yet the anomalous backscatter only occurs at the anticlinal crest region. Away from the faults the anticlinal ridge crest shows no anomalous backscatter.

A piston core was deployed into the center of the anomalous backscatter patch on the anticlinal ridge crest. A sub-bottom profile line acquired by the coring vessel, oriented SE-NW, shows seafloor-parallel reflectors outside of the anomalous backscatter area trending into an area of diffracted energy and irregular seafloor (Figure 11c). This core recovered 4.88 m of high cohesion, moderate water content dark green gray clay, with a good H_2S odor near the base of the core and shell fragments within the core. The presence of an H_2S odor indicates that the core has penetrated well into the sulfate reduction zone (through the oxidized region below the mud line), so that any hydrocarbons that have migrated through the section have a lower risk of biodegradation.

This core yielded a hydrocarbon hit (both oil and gas) based upon TDI's threshold values. Two other cores in the area brought back evidence of gas. A TGS seismic line in the area shows an extremely strong BSR, with some stratal brightening below it, and possible crestal faults that could facilitate hydrocarbon migration through the hydrate stability field for the northwestern pair of geochemical hits (e.g., Trehu et al., 2004). For the oil and gas hit shown in Figure 11b-d, we suggest that the along-strike strain variation associated with a single anticline projecting into two anticlines resulted in minor high angle strike-slip faulting, and that the combination of high angle faults and the crest of the anticline facilitates hydrocarbon migration from the sub-surface to the seafloor.

Furthermore, seepage may not be active today, but was present in this area in the past as evidenced by the shell fragments located 4.8 m below the top of the core. We propose that it is the presence of these shell fragments that, although buried, cause the increase in backscatter through an increase in volumetric scattering below the mud line (Gardner et al., 1991; Kenyon, 1992).

There are many examples of the association of high backscatter with buried (relict) seepage in the IndoDeep program. This demonstrates that multibeam is sensitive to the geologic record of seepage in the upper approximate 10 m of the sedimentary section, that cores to such features can recover measurable hydrocarbons, and therefore that multibeam (in contrast to tools such as ALF and SAR) does not require seepage to be occurring at the time of sampling to successfully yield information on a basin's petroleum system.

High Backscatter Patch with No Bathymetric Expression

A third feature identified in the Misool survey area was a patch of anomalously high backscatter approximately 200 m across on a relatively uniformly sloping seafloor ridge with no local bathymetric anomaly associated with the backscatter (Figure 12a, b). A sub-bottom profiler line, oriented SE-NW across the feature, showed there to be no significant variations in local seafloor relief that would lead to diffractions, and faint but identifiable reflectors parallel to the seafloor trending into the anomaly region (Figure 12c). In the region of anomalous backscatter no sub-surface reflectors are identifiable, but instead there appear several strong diffractions and a patchy high reflectivity appearance to the sub-surface. A core deployed to the center of this feature recovered 1.82 m of dark gray sticky clay with numerous authigenic carbonate fragments and a H_2S odor. A nodule of gas hydrate was observed near the base of the core, which was extracted and allowed to dissociate in clean seawater into a headspace gas can for an additional geochemical analysis from this core (Figure 12d). Initial geochemical analyses of this core indicate a mixed thermogenic and biogenic gas source. More recent detailed analysis of the core indicates an oil signature as well.

DISCUSSION

Modern multibeam systems are now capable of imaging natural hydrocarbon seep features relevant to petroleum exploration, and moreover, can do so at survey speeds of about 18.5 km/hr (10 knots), in water depths up to 4000 m deep. Such data are, however, not routine, and require extensive attention to detail to all aspects of the survey platform, including detailed surveying in of the multibeam array itself, the DGPS system, and the motion reference unit, with additional loop ties between all systems carried out until the errors are

within a range acceptable for exploration (note that this is a much more rigorous specification than standard hydrographic surveys). Through survey design, system calibration, execution, and the detailed and continuous evaluation of every aspect of the acquisition system, we are able to image seafloor features on the order of 10-100 m in lateral dimension, with less than 5 m vertical relief, on the seafloor in up to 3000 m of water. The SeaSeep grids and mosaics created as part of the IndoDeep program have a bathymetric cell size of 25 m and a backscatter pixel of 5 m, independent of water depth. Over 1000 sq km of quality data can be acquired on a daily basis, with final seafloor maps and mosaics delivered upon the completion of each cruise leg. This allows for rapid integration with existing data, and identification of targets relevant to the petroleum system.

The ability to map the seafloor at very high resolution, both bathymetrically and with georeferenced and quantitative acoustic backscatter, allows for the identification of anomalous seafloor features that may be related to natural hydrocarbon seepage. To interrogate these potential seep sites, we deploy a standard 6 m – 9 m piston corer equipped with a Ultra-Short BaseLine (USBL) positioning beacon so that the core can be tracked in three dimensions all the way to the seafloor target.

CONCLUSIONS

The SeaSeep exploration technique was applied to the IndoDeep multi-client project offshore Indonesia, which acquired 400,000 sq km of multibeam bathymetry and backscatter data, 100,000 line km of gravity and magnetics, 1182 piston cores for geochemical analysis, and 34,000 line km of new 2D seismic data. The geochemical analyses showed that 12% of the cores contain migrated liquid petroleum, and 44% contain thermogenic gas. Over 400 isotope pairs, and over 60 biomarker (molecular fingerprinting) suites provide insight into the maturity and source of multiple gas and oil petroleum systems.

Over 90% of the successful geochemical 'hits' are associated with anomalously high backscatter. The strength of the geochemical anomaly, however, was in part related to the target type (Figure 13), with mud volcanoes yielding the largest geochemical anomalies related to seepage. Mud volcanoes, however, were not present in every survey area, and were distributed unevenly even in the sub-areas where they were found. Faults and anticlines also
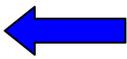
provided relatively strong seepage, but only at target sites that were characterized by local anomalous high backscatter on the geologic feature. In areas that had no geologic conduit that could create anisotropic permeability or that brought overpressured material directly to the surface, seep features occur as patches of anomalous backscatter on an otherwise monotonous seafloor.

Cores that successfully retrieve hydrocarbons from such features can provide a wealth of information into the subsurface hydrocarbon system in an area where it would otherwise be impossible to interrogate it. Even though such seep signatures are relatively weak, they have a disproportionate impact on exploration because they provide petroleum system information (and actual geochemical data) in low seepage areas that may have had no previous indications of a viable hydrocarbon system.

In order to understand the impact of the seafloor cores and geochemistry on exploration prospectivity, the explorationist must first determine what the seafloor target was, tie the target type to the geochemical results, compare these results with similar targets in that area, compare (or contrast) the results with different target types in that area, and then, finally, extrapolate the geochemical insights from this target type to other similar targets in the field area that may not have been sampled.

The success of the IndoDeep program significantly impacted the exploration risk in all of the survey areas by providing valuable information on source, maturity and migration. The integration of the SeaSeep results with interpretation of the 2D seismic data allowed BGE to high-grade areas for further exploration, focusing efforts (and future exploration dollars) on the most prospective areas within the larger survey program. SeaSeep results have lead to the recognition of active petroleum systems in areas where they were not thought to be present, and the recognition of petroleum systems that have not been identified previously in Indonesia. Black Gold's recent exploration activities in Indonesia demonstrate the business case for SeaSeep as a cost effective tool for rapid risk reduction in frontier exploration.

Combined with more traditional data sets such as 2D seismic, gravity and magnetics, multibeam surveys and follow-up navigated coring can be used to lower the risk for exploration by providing information on source, migration, maturity and charge. A well-planned and well-executed SeaSeep survey can rapidly, efficiently and effectively

identify and sample oil and gas seeps in frontier basins.

ACKNOWLEDGEMENTS

REFERENCES CITED

Bernard, B.B., Brooks, J.M., Baillie, P., Decker, J., Teas, P.A., and Orange, D.L., 2008, Surface Geochemical Exploration and Heat Flow Surveys in Fifteen (15) Frontier Indonesia Basins: Proceedings, Indonesia Petroleum Association, IPA08-G-210, 14 pp.

Christoffel, D.A. and Calhaem, I.M., 1969, A geothermal heat flow probe for in situ measurement of both temperature gradient and thermal conductivity: J. Phys. E: Sci. Instrum,. v. 2, p. 457-465 doi: 10.1088/0022-3735/2/6/301

Fleisher, P., Orsi, T.H., Richardson, M.D., and Anderson, A.L., 2001, Distribution of free gas in marine sediments: a global overview: Geo-Marine Letters, v. 21, p. 103-122.

Fonseca, L., Mayer, L., Orange, D., and Driscoll, N., 2002, The high-frequency backscattering angular response of gassy sediments: Model/data comparisons from the Eel River margin, California: J. Acoust. Soc. Am., v. 111, p. 2621-2631.

Gardner, J.V., M.E. Field, H. Lee, B. Edwards, D.G. Masson, N. Kenyon, and R.B. Kidd, 1991, Ground-truthing 6.5 kHz side scan sonographs: what are we really imaging?: Journal of Geophysical Research, v. 96, p. 5955-5974.

Hovland, M., and Judd, A.G., 1988, Seabed Pockmarks and Seepages: Impact on Geology, Biology and the Marine Environment: London, Graham and Trotman Ltd., 293 pp.

Hyndman R.D., and Spence, G.D., 1992, A Seismic Study of Methane Hydrate Marine Bottom Simulating Reflectors: Journal of Geophysical Research, v. 97, p. 6683-6698.

Judd, A.G., and Hovland, M., 2007, Seabed Fluid Flow: The Impact on Geology, Biology and the Marine Environment. London: Cambridge University Press, 492 pp.

Kennicutt II, M.C., Brooks, J.M., Bidgare, R.R., Fay, R.R., Wade, T.L., and McDonald, T.J., 1985, Vent-type taxa in a hydrocarbon seep region on the Louisiana Slope: Nature, v. 317, p. 351-353.

Kenyon, N.H. 1992, Speculations on the geological causes of backscatter variation on GLORIA sonographs from the Mississippi and De Soto fans, Gulf of Mexico: Geo-Marine Letters, v. 12, p. 24-32.

Kulm, L.D., Suess, E., Moore, J.C., Carson, B., Lewis, B.T., Ritger, S.D., Kadko, D.C., Thornburg, T.M., Embley, R.W., Rugh, W.D., Massoth, G.J., Langseth, M.G., Cochrane, G.R., and Scamman, R.L., 1986, Oregon Subduction Zone: Venting, Fauna, and Carbonates: Science, v. 231, p. 561-566.

Le Pichon, X., Foucher, J.P., Boulegue, J., Henry, P., Lallement, S., Benedette, M., Avedik, F., and Mariotti, A., 1990, Mud Volcano Field Seaward of the Barbados Accretionary Complex – a

Submersible Study: Journal of Geophysical Research, v. 95, p. 199-213.

Mayer, L. A., 2006. Frontiers in Seafloor Mapping and Visualization: Marine Geophysical Researches., v. 27, p. 7–17. DOI 10.1007/s11001-005-0267-x

MacDonald, I.R., G.S. Boland, J.S. Baker, J.M. Brooks, M.C. Kennicutt II, and R.R. Bidigare, 1989, Gulf of Mexico Chemosynthetic Communities II: Spatial Distribution of Seep Organisms and Hydrocarbons at Bush Hill: Marine Biology, v. 101, p. 235-247.

McConnell, D.R., and Kendall, B.A., 2002, Images of the Base of Gas Hydrate Stability, Northwest Walker Ridge, Gulf of Mexico: Proceedings, Offshore Technology Conference, Houston, 6-9 May 2002, OTC paper #14103.

Mosher, D.C., 2008, Bottom Simulating Reflectors on Canada's East Coast Margin: Evidence for gas hydrate: Proceedings of the 6th International Conference on Gas Hydrates (ICGH 2008), Vancouver, British Columbia, Canada, July 6-10, 2008. 11 pp.

Noble, R., Orange, D., Decker, J., Teas, P.A., and Baillie, P., 2009, Oil and Gas Seeps in Deep Marine Sea Floor Cores as Indicators of Active Petroleum Systems in Indonesia: Proceedings, Indonesia Petroleum Association (this volume).

Orange, D.L. and Breen, N.A., 1992, The Effects of Fluid Escape on Accretionary Wedges II: Seepage Force, Slope Failure, Headless Submarine Canyons and Vents: Journal of Geophysical Research, v. 97, 9277-9295.

Orange, D.L., H.G. Greene, D. Reed, J.B. Martin, C.M. McHugh, W.B.F. Ryan, N. Maher, D. Stakes, and J. Barry, 1999, Widespread Fluid Expulsion on a Translational Continental Margin: Mud Volcano, Fault Zones, Headless Canyons, and Aquifers in Monterey Bay, California: Geological Society of America Bulletin, v. 111, p. 992-1009.

Orange, D.L., Yun, J., Maher, N., Barry, J., and Greene, G., 2002, Tracking California Seafloor Seeps with Bathymetry, Backscatter and ROVs: Continental Shelf Research, v. 22, p. 2273-2290.

Orange, D.L., Teas, P.A., Decker, J., Baillie, P., Gilleran, P., and Levey, M.D., 2008, The Utilisation of SeaSeep Surveys (a Defense / Hydrography Spin-Off) to Identify and Sample Hydrocarbon Seeps in Offshore Frontier Basins: International Petroleum Technology Conference, IPTC-12839, 17 pp.

Robb, J.M., 1984, Spring Sapping on the Lower Continental Slope, Offshore New Jersey: Geology, v. 12, p. 278-282.

Robb, J.M., 1990, Groundwater Processes in the Submarine Environment. In Coates, D.R., ed., Groundwater Geomorphology: The Role of Subsurface Water in Earth Surface Processes and Landforms: Geological Society of America Special Paper no. 252, p. 267-282.

Roberts, H.H., P. Aharon, R. Carney, J. Larkin, and R. Sassen, 1990. Seafloor Responses to Hydrocarbon Seeps, Louisiana Continental Slope: Geo-Marine Letters, v. 10, p. 232-243.

Sager, W.W., I.R. MacDonald, and R. Hou, 2003, Geophysical Signatures of Mud Mounds at Hydrocarbon Seeps on the Louisiana Continental Slope, Northern Gulf of Mexico: Marine Geology, v. 198, p. 97-132.

Sager, W.W., I.R. MacDonald, and R. Hou, 2004, Side-Scan Sonar Imaging of Hydrocarbon Seeps on the Louisiana Continental Slope: American Association of Petroleum Geologists Bulletin, v. 88, p. 725-746.

Shipley, T.H., Houston, M.H., Buffler, R.T., Shaub, F.J., McMillen, K.J., Ladd, J.W., and Worzel, J.L., 1979, Seismic Evidence for the Widespread Occurrence of Possible Gas-hydrate Horizons on Continental Slopes and Rises: American Association of Petroleum Geologists Bulletin, v. 63, p. 2204-2213.

Somoza, L., Diaz-del-Rio, V., Leon, R., Ivanov, M., Fernandez-Puga, M.C., Gardner, J.M., Hernandez-Molina, F.J., Pinheiro, L.M., Rodero, J., Lobato, A., Maestro, A., Vazquez, J.T., Medialdea, T., and Fernandez-Salas, L.M., 2003, Seabed Morphology and Hydrocarbons in the Gulf of Cadiz Mud Volcano Area: Acoustic Imagery, Multibeam, and Ultrahigh Resolution Seismic Data: Marine Geology, v. 162, p. 153-176.

Steinberg, B.D., 1976, Principles of Aperture and Array System Design (Ch. 7): John Wiley & Sons, Wiley Interscience Publ., 356 pp.

Stutzman, W.L., and Thiele, G.A., 1981, Antenna Theory and Design: John Wiley & Sons, 1981, 608 pp.
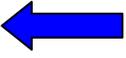
Suess, E., Carson, B., Ritger, S.D., Moore, J.C., Jones, M.L., Kulm, L.D., and Cochrane, G.R., 1985, Biological Communities at Vent Sites Along the Subduction Zone off Oregon: Bulletin Biology Society of Washington, v. 6, p. 475-484.

Trehu, A.M, Flemings, P.B., Bangs, N.L., Chevallier, J., Gracia, E., Johnson, J.E., Liu, C.-S., Liu, X., Riedel, M., and Torres, M.E., 2004, Feeding Methane Vents and Gas Hydrate Deposits at South Hydrate Ridge: Geophysical Research Letters,v. 31, L23310, doi:10.1029/2004GL021286.

Von Herzen, R.P. and Anderson, R.N., 1972, Implications of Heat Flow and Bottom Water Temperature in the Eastern Equatorial Pacific: Geophys. J. R. Astr. Soc., 26, 427-459.

Westbrook , G., Exley, R., Minshull, T., Nouzé, H., Gailler, A., Jose, T., Ker, S., and Plaza, A., 2008, High-resolution 3D Seismic Investigations of Hydrate-bearing Fluid-Escape Chimneys in the Nyegga Region of Vøring Plateau, Norway: Proceedings of the 6th International Conference on Gas Hydrates (ICGH 2008), Vancouver, British Columbia, Canada, 12 pp.

Xu W., and Ruppel C., 1999, Predicting the Occurrence, Distribution and Evolution of Methane Gas Hydrate in Porous Marine Sediments: Journal of Geophysical Research, v. 104, p. 5081-5095.

Zwart, G., Moore, J. C., Cochrane, G. R., 1996, Variations in Temperature Gradients Identify Active Faults in the Oregon Accretionary Prism: Earth and Planetary Sciences Letters, v. 139, p. 485-495.
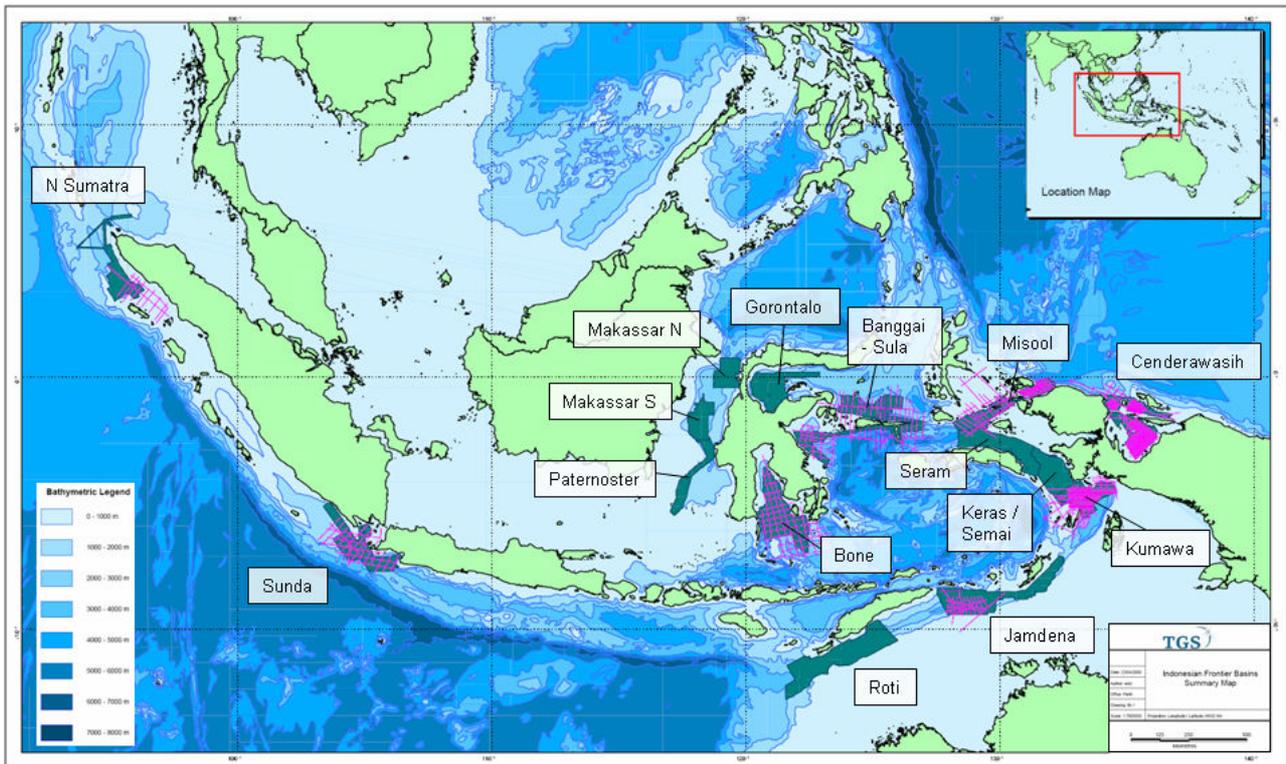
Figure 1 - Regional map of Indonesia showing TGS IndoDeep multi-client program area. Multibeam bathymetry and backscatter surveys shown by green polygons. Magenta lines represent new 2D multi-channel seismic data.
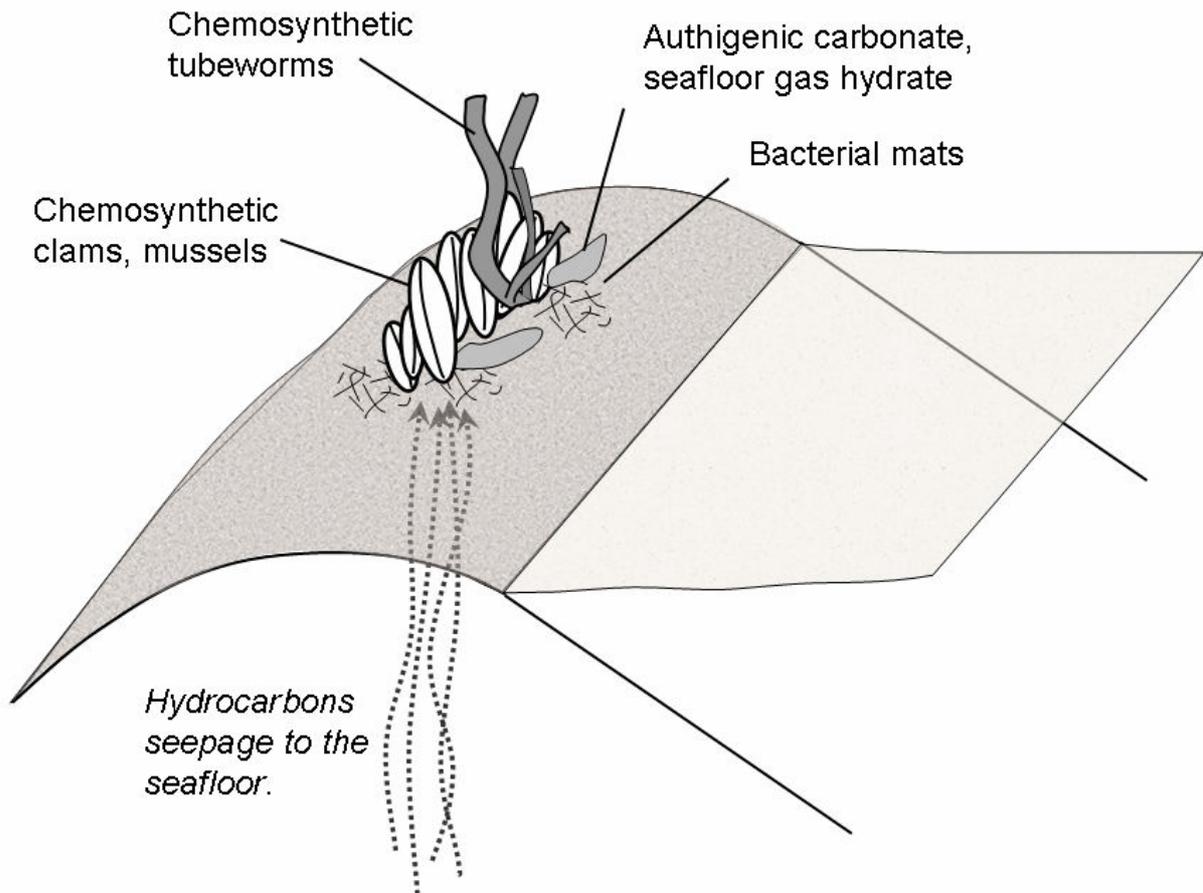
Figure 2 - Schematic illustration of seafloor hydrocarbon seep with chemosynthetic community. Bacteria and other organisms metabolize seeping hydrocarbons facilitating precipitation of authigenic carbonate and other precipitates, and also form the base of the food chain for seep fauna. Precipitates and seep fauna can be detected with mulitbeam surveys.
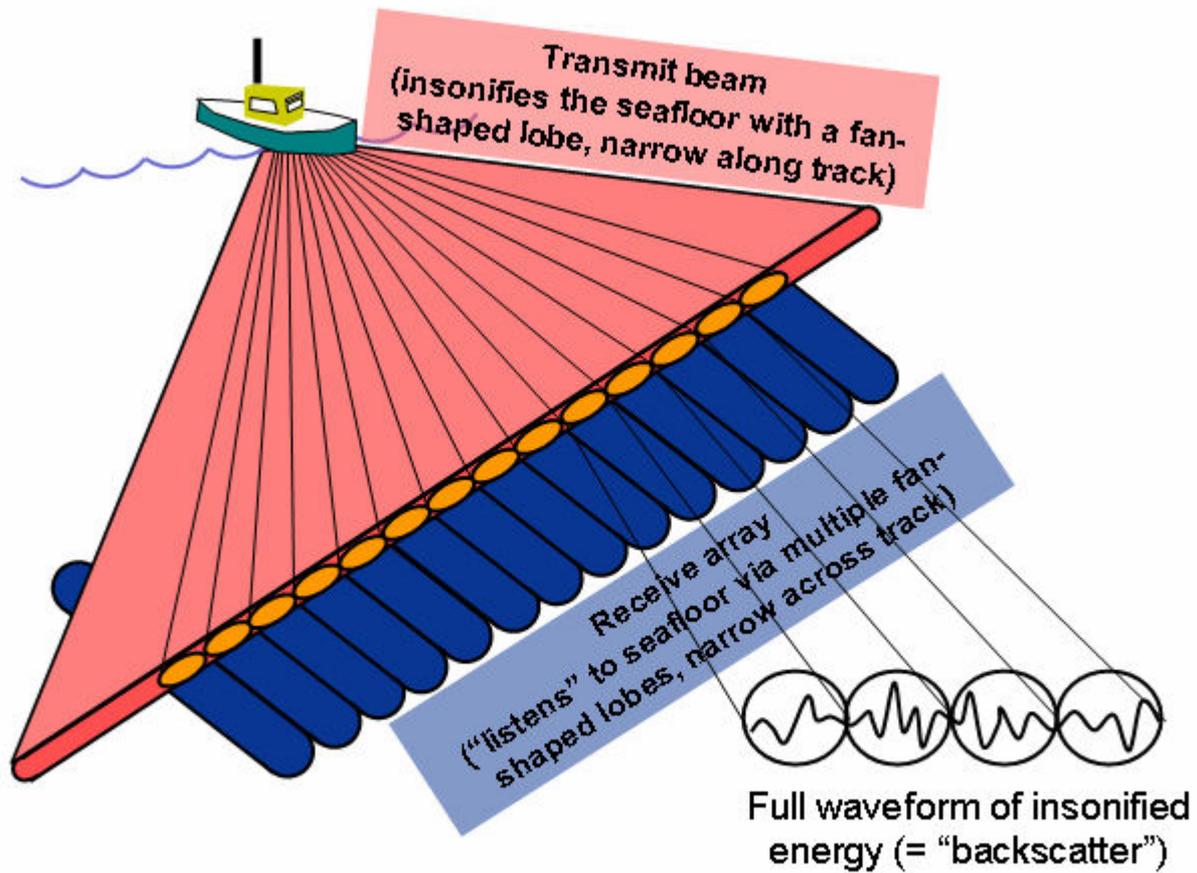
Figure 3 - Diagram illustrating multibeam acquisition using orthogonal transducer arrays. The transmit array (oriented parallel to the ship's keel) insonifies the seafloor with a fan-shaped lobe which is narrow along track. The receive array, oriented athwartship, "listens" to the seafloor via multiple fan-shaped lobes which are narrow across track. Each "beam" represents the intersection of the transmit array energy recorded by the receive array. **The location of each beam on the seafloor is calculated based on the two-way travel time, the location and position of the ship at the time of transmit and the time of receive, corrected for refraction in the water column.** The full waveform of return energy ("backscatter") is measured for each accurately located beam and corrected, resulting in georeferenced quantitative backscatter.
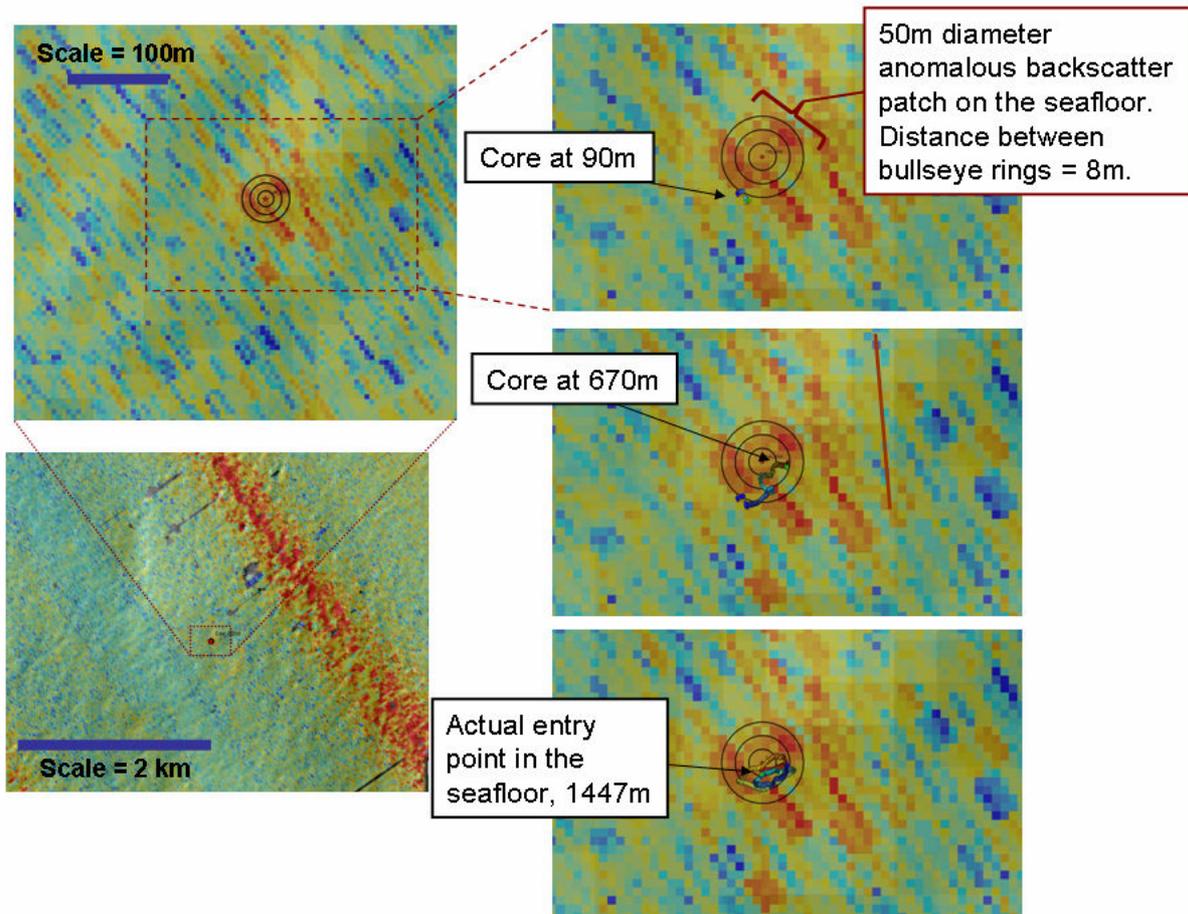
Figure 4 - Real time core position monitoring insures precise core placement necessary to sample small seafloor features. A USBL beacon on the core is continuously monitored to track the core as it descends through the water column, as shown here at 90, 670 and 1447 m water depths.
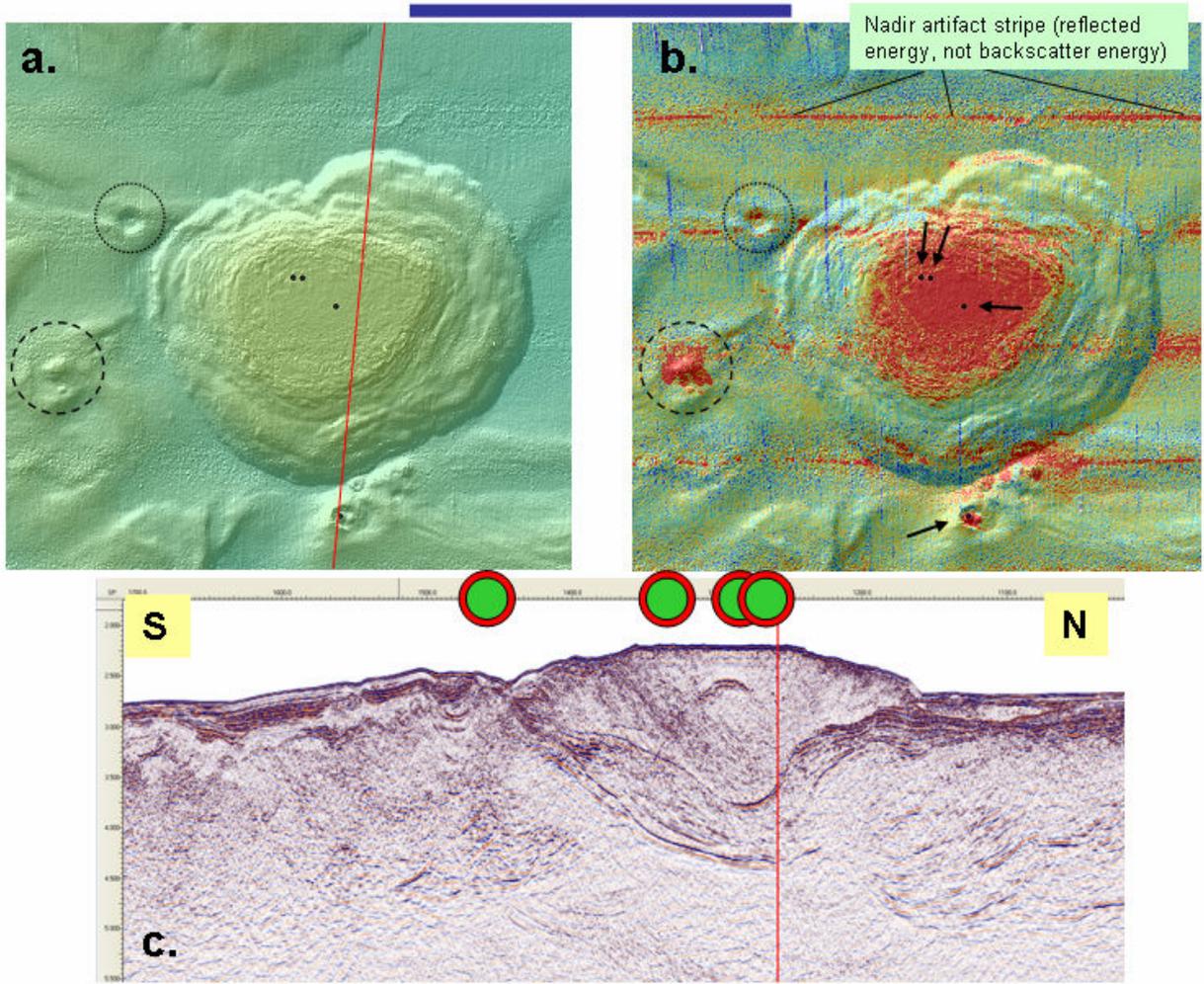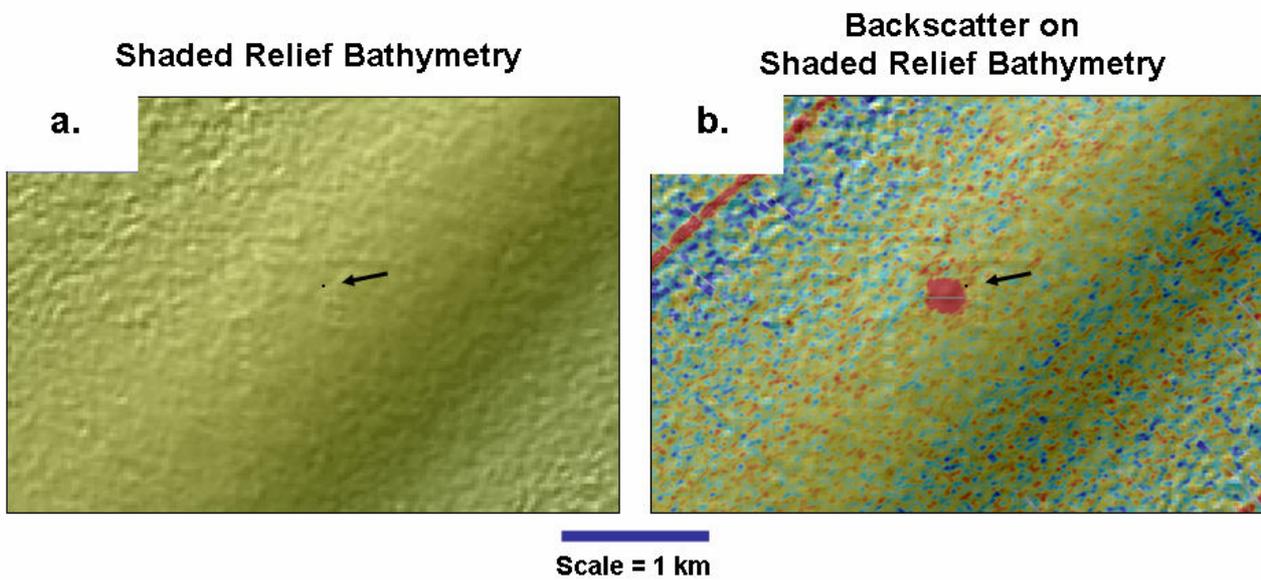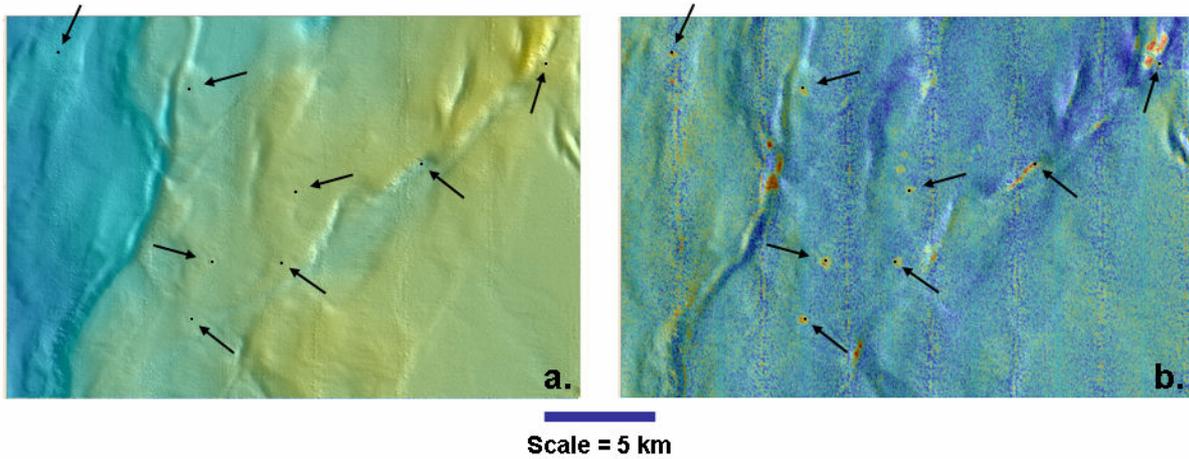
Figure 5 - Shaded relief bathymetry (a) with backscatter drape (b) and seismic line (c) of the Raksasa mud volcano. Areas of high backscatter shown in red. Other features described in text include pockmark to the NW (dashed circle) and a small mud volcano to the south (arrow). Locations of four cores shown by black dots with arrows (b). Location of seismic line shown by red line in (a) with projected locations of cores with anomalous geochemistry shown by red [gas] and green [oil] circles (c).
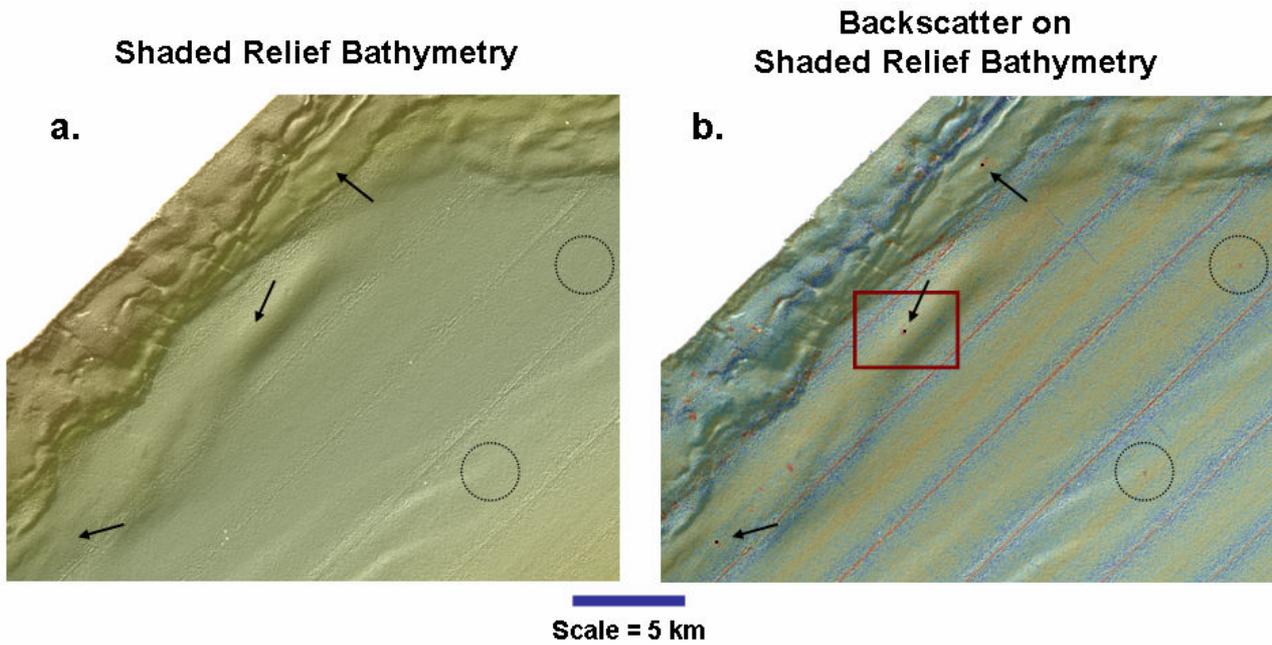
Figure 6 - Shaded relief bathymetry (a) with backscatter drape (b) of a portion of the Taninbar Trough. Circular small high backscatter patches (circled and at arrows) occur at an anticlinal ridge crest (red rectangle) and on featureless seafloor. Location of cores shown by black dots with arrows.
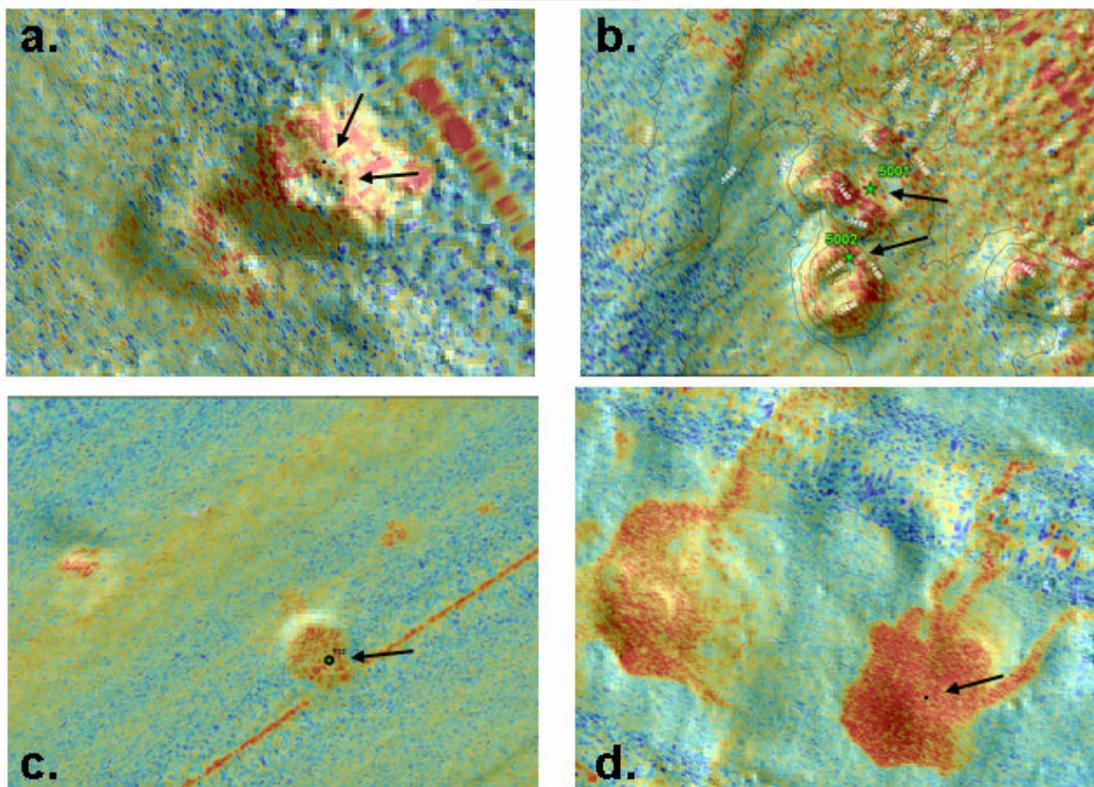

Figure 7 - Shaded-relief bathymetry (a) with backscatter drape (b) on the NE-SW trending anticline shown in Figure 6. High backscatter (red color on b) occurs as circular patches with no associated bathymetric relief. Geochemical analysis from this core target (dot at arrow) yielded thermogenic gas.

Scale = 5 km

Figure 8 - Shaded relief bathymetry (a) with backscatter drape (b) of a portion of the Makassar North survey area. Potential seafloor targets occur as circular anomalous backscatter patches with no anomalous relief, as high backscatter lineations along portions of faults with seafloor expression, and as a patch of anomalous backscatter on a hanging-wall anticline associated with NW-vergent faulting. Piston cores locations shown by arrows. 6 of the 8 cores yielded evidence of thermogenic hydrocarbons, with consistent signatures within target types, but differences between the target types.

Scale = 1 km

Scale = 1 km

Figure 9 - Shaded relief bathymetry with backscatter drape (c-d) on four mud volcanoes imaged in the IndoDeep survey program. The location of cores is shown by arrows. All four mud volcanoes yielded evidence of thermogenic hydrocarbons; three of the four yielded sufficient hydrocarbon material for biomarker fingerprinting.
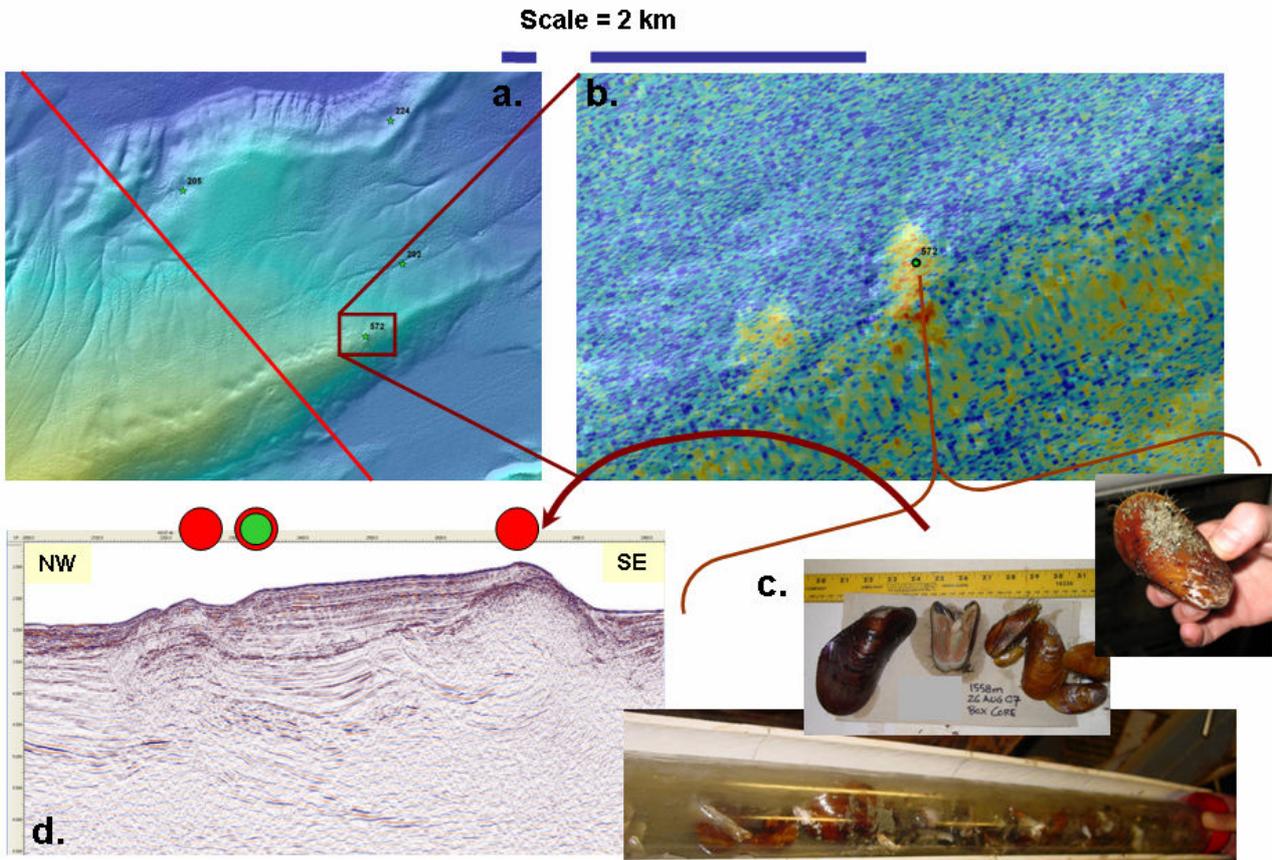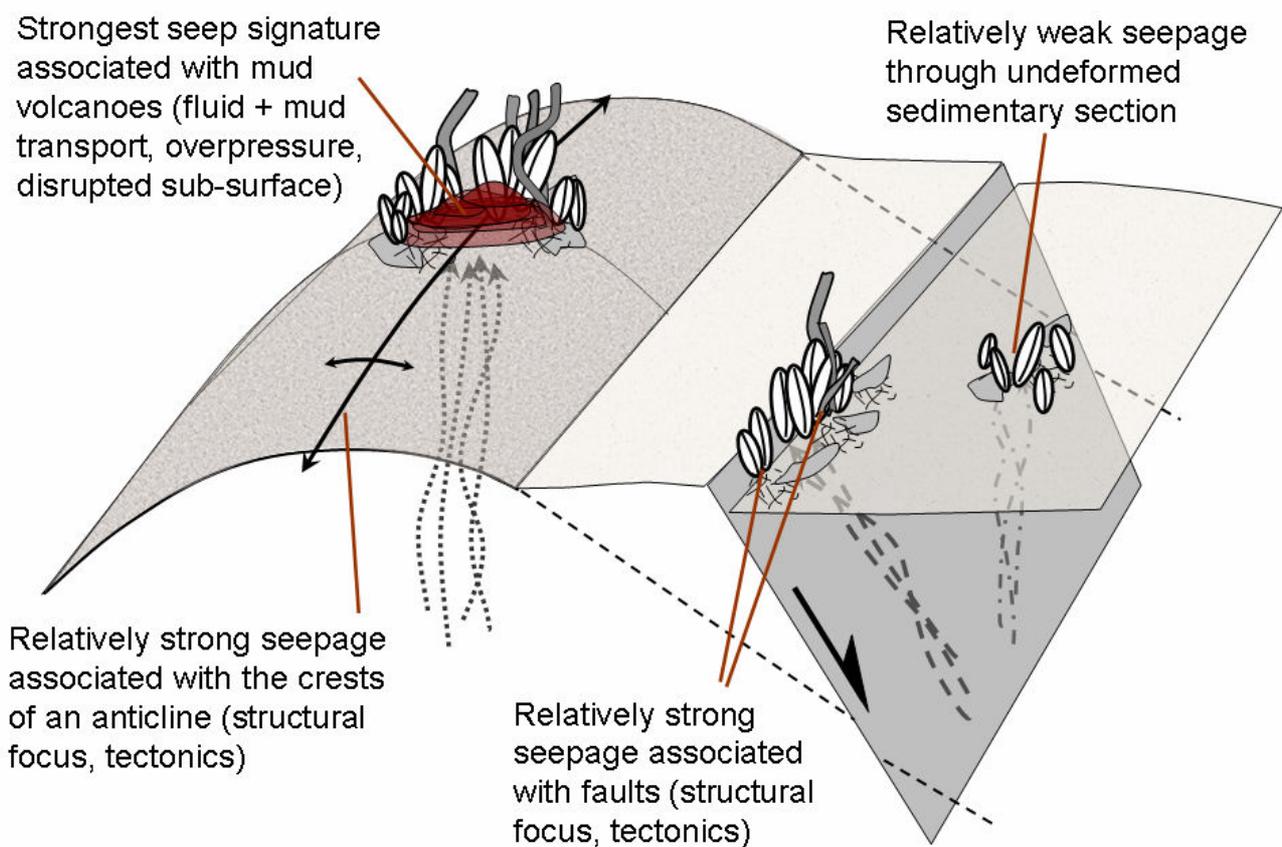
Figure 10 - Shaded relief bathymetry (a) with backscatter drape of enlarged area (b) and seismic profile (d) of ridge top anomalous backscatter site at NE Misool. Anomalously high backscatter patches up to several hundred meters across occur with no to minor local mounding. A piston core into the backscatter anomaly shown by green star (a) and green dot (b) contained live mussels and shell fragments (c), and authigenic carbonate.
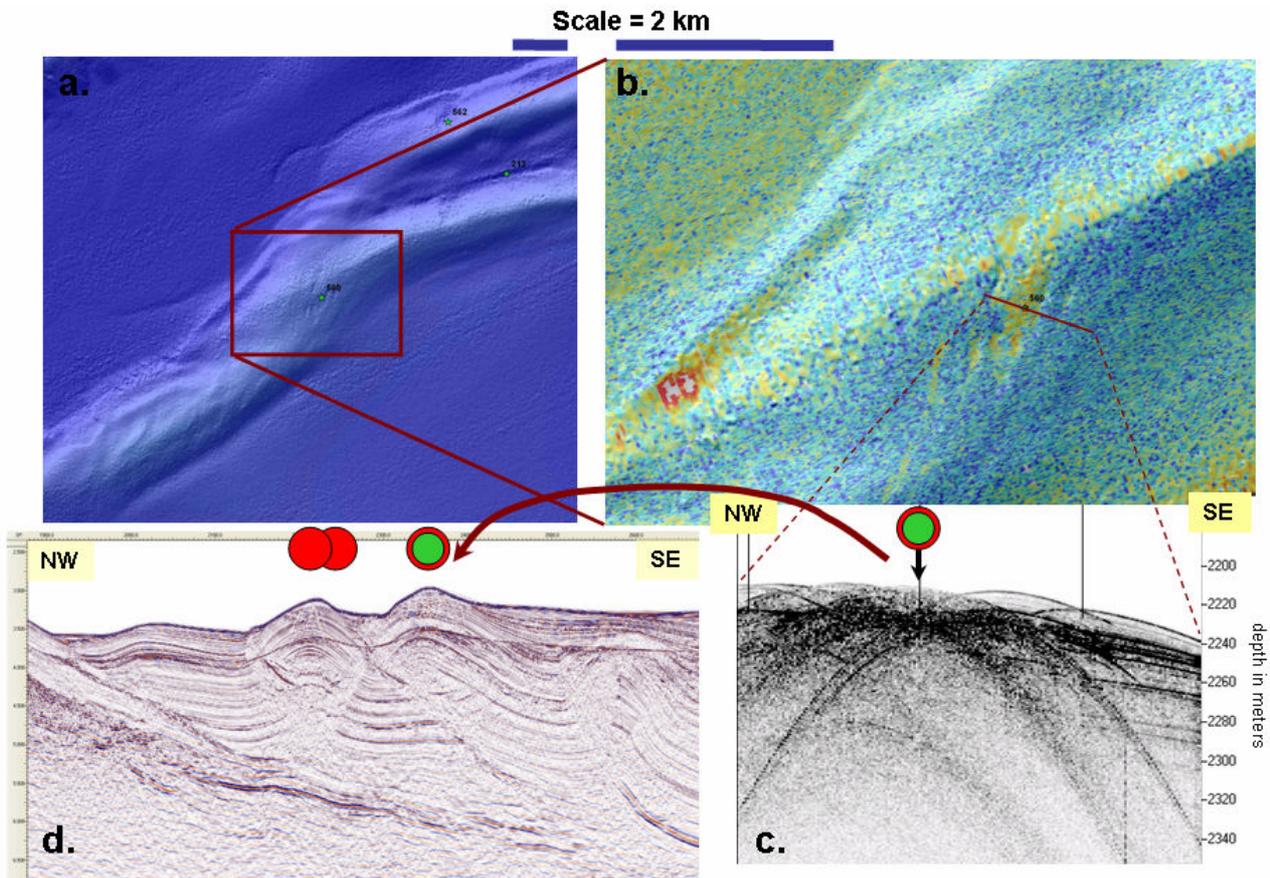
Figure 11 - Shaded relief bathymetry (a) with backscatter drape of enlarged area (b) illustrating high angle tear faults on crest of an anticline in NE Misool. Note backscatter anomalies associated with NE-trending lineations only at the crest of the anticline (b). A SE-NE sub-bottom profile (c) shows disruption of seafloor sub-parallel reflectors in the anomalous backscatter area. A piston core from the anomalous backscatter region yielded evidence of both oil and gas. Local brightening below observed a strong BSR from a regional seismic line near the core location (d) is interpreted as shallow gas accumulations below the gas hydrate stability field along the anticline crests. The faults observed at the seafloor (both crestal extensional faults, and lateral strain accommodation faults) likely provide migration pathways for detected hydrocarbon seeps.
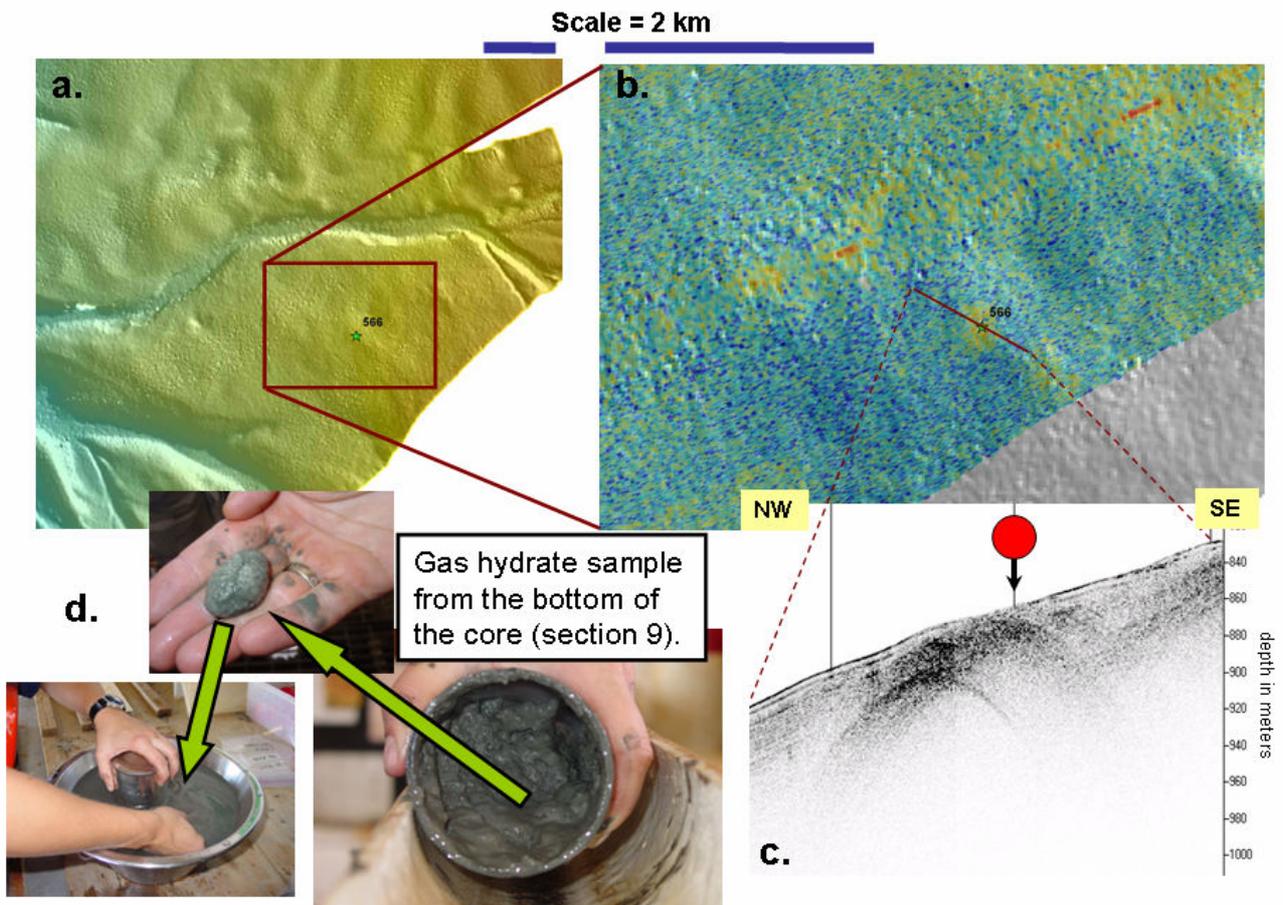
Figure 12 - Shaded relief bathymetry (a) with backscatter drape of enlarged area (b) illustrating anomalous high backscatter patch in an area with no local bathymetric anomaly, NE Misool. A sub-bottom profile line (c) over the feature reveals a smooth seafloor surface underlain by diffractions, and strong but irregular returns. A core from the center of this feature yielded gas hydrates (d). Gas dissociated from the hydrates was collected in headspace gas cans (d). Geochemical analyses of this core also yielded evidence of thermogenic hydrocarbons.

Strongest seep signature associated with mud volcanoes (fluid + mud transport, overpressure, disrupted sub-surface)

Relatively weak seepage through undeformed sedimentary section

Relatively strong seepage associated with the crests of an anticline (structural focus, tectonics)

Relatively strong seepage associated with faults (structural focus, tectonics)

Figure 13 - Seafloor hydrocarbon seep model. Mud volcanoes transport both fluid and mud to the seafloor, and have the strongest seep signatures. Relatively strong seafloor seep signatures can be associated with anticlinal crests and with faults. Seep strength in undeformed regions of the seafloor is weak, as it is difficult to migrate fluids through competent sediment layers. Although such seep signatures may be weak, they carry disproportionate impact because they may provide information about the areal distribution of the hydrocarbon system in a previously unknown basin with no other obvious (or easily imaged) seafloor targets.